



The use of recycled materials in a biofilter to polish anammox wastewater treatment plant effluent



Debojit S. Tanmoy ^{a,b,c}, Juan C. Bezares-Cruz ^c, Gregory H. LeFevre ^{a,b,*}

^a Department of Civil and Environmental Engineering, University of Iowa, 4105 Seamans Center, Iowa City, IA, 52242, United States

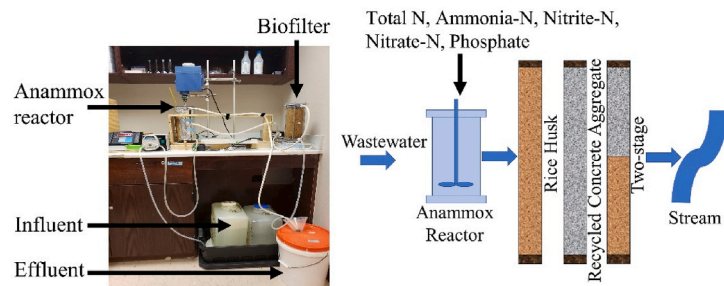
^b IHR—Hydroscience and Engineering, University of Iowa, 100 C. Maxwell Stanley Hydraulics Laboratory, Iowa City, IA, 52242, United States

^c Department of Environmental Engineering, Texas A&M University—Kingsville, MSC 213, 925 W. Avenue B, Kingsville, TX, 78363, USA

HIGHLIGHTS

GRAPHICAL ABSTRACT

- Anammox treated wastewater requires further polishing due to high nutrient loads.
- Two-stage biofilter can remove nutrients and be used for effluent polishing.
- Rice husks facilitate biofilm growth and can efficiently remove N nutrients.
- Recycled concrete aggregates have higher P sorption capacities ($q_{\max} = 0.074 \text{ mg/g}$).
- First study to investigate recycled materials to polish anammox effluent.



ARTICLE INFO

Handling Editor: Y Yeomin Yoon

Keywords:

Anammox
Effluent polishing
Recycled materials
Biofilter
Adsorption
Nutrient pollution

ABSTRACT

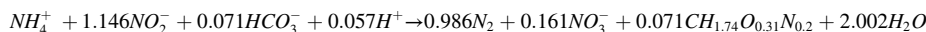
Anammox is gaining popularity for treating wastewater containing high-strength ammonia due to lower energy demand compared to conventional nitrification-denitrification processes; however, anammox is reported to increase nitrate loads in the effluent. The objective of this study was to assess the applicability of recycled materials [recycled concrete aggregate (RCA) and rice husks (RH)] as a polishing step to improve anammox reactor effluent quality. Anammox effluents were separately passed through two single-stage columns containing RCA and RH, and one two-stage column (50% RCA, 50% RH) to quantify total N, ammonia, nitrate, nitrite, and phosphate removal efficiencies. Langmuir isotherm experiments were conducted to quantify nitrate, nitrite, and phosphate sorption capacities in the columns. The RCA column exhibited the highest phosphate sorption capacity (0.074 mg/g), while the RH column exhibited higher nitrite and nitrate adsorption (0.063 mg/g and 0.023 mg/g respectively). We created a Hydrus-1D model to estimate pseudo-first-order reaction rates in the columns. Because RCA media can form metal-phosphate precipitates, the fastest phosphate reaction rate (1.58 min^{-1}) occurred in the RCA column. The two-stage column demonstrated the greatest overall removals for all nutrients, and removal rates were consistent throughout the experimental period. The two-stage column achieved 15% total N, 94% ammonia-N, 38% nitrate-N, 75% nitrite-N, and 27% phosphate removal. The maximum nitrite, nitrate, and phosphate adsorption capacities in the two-stage column were 0.030 mg/g, 0.017 mg/g, and 0.014 mg/g respectively. This is the first study to demonstrate that recycled materials can successfully be integrated into a biofilter as an effluent polishing step to remove nutrients from anammox wastewater.

* Corresponding author. Seamans Center for Engineering, University of Iowa, Iowa City, IA, United States.

E-mail address: gregory-lefevre@uiowa.edu (G.H. LeFevre).

1. Introduction

Eutrophication of surface waters is a global challenge (EPA, 2009) that degrades aquatic life, increases water treatment costs (Piper, 2003), and contributes to algal blooms that produce toxins (Yang et al., 2008). Indeed, the U.S. faces an estimated annual economic loss of 2.2 billion USD due to freshwater eutrophication (Dodds et al., 2009). Conventionally, nitrification/denitrification processes in wastewater treatment plants (WWTPs) are used to ameliorate nitrogen loads in the effluent; unfortunately, these processes are energy-intensive. Aeration is the most energy-consuming process, using 13–77% of the total 0.26 to 1.6 kWh needed to treat every cubic meter of water, and consequently accounts for 45–75% of the total operational cost of the treatment plan (Maktabifard et al., 2018; Rosso et al., 2008). Conventional wastewater treatment plants are also responsible for significant greenhouse gas production (Gude, 2015). A relatively recent innovative technology to treat nitrogen-rich wastewater is anaerobic ammonium oxidation (anammox) (Lotti et al., 2014) (Equation (1)):



Equation 1

Anammox is becoming increasingly popular because the process does not require aeration and thus substantially lowers energy usage and operational cost. Anammox is reported to lower energy usage by 65% and eliminate the use of external carbon sources compared to conventional nitrification and denitrification processes (Gude, 2015). Anammox is also being considered in stormwater treatment technologies where it is applied after a partial nitritation process (Sun et al., 2017). Nevertheless, although anammox lessens the total N load, the anammox process is reported to increase nitrate concentration in the effluent (Si et al., 2021). The anammox reaction is also inhibited by high influent phosphate concentration (when influent $PO_4^{3-}-P \geq 160$ mg/L) (Si et al., 2021). If influent nitrogen concentrations are high, high effluent nitrate concentrations also result (Daverey et al., 2013); thus, additional polishing of anammox effluent is necessary before discharge (Conley et al., 2009; Preisner et al., 2020)—particularly as discharge limits are expected to lower over time.

Traditional treatment plants sometimes employ effluent polishing processes to improve the quality of effluent that reaches surface waters. Supplementary polishing is generally practiced if the wastewater effluent is used for irrigation or is discharged into a waterbody used as a recreational and drinking water source (Ameta, 2018; Gerba and Pepper, 2019). Examples of effluent polishing operations include waste stabilization ponds, vegetative uptake, rapid filters, lagoons, constructed wetlands, woodchip bioreactors, and wood-iron bioreactors, which can sometimes require large areas of land (Toet et al., 2005; Verlicchi et al., 2011; Yamashita and Yamamoto-Ikemoto, 2014). Constructed wetlands have become widely-used to treat and improve final municipal wastewater effluent (Brown et al., 2000). Constructed wetlands can decrease nitrogen, phosphorus, pathogens, pharmaceuticals, and trace organic contaminant levels in municipal wastewater effluent via biotransformation, photo-transformation, and adsorption onto wetland matrices (Jasper et al., 2013, 2014; Jasper and Sedlak, 2013; Oulton et al., 2010; Scholes et al., 2021). Wetlands have also been used to polish reverse osmosis concentrate generated from municipal WWTPs (Scholes et al., 2021). Biofilters made with media of recycled materials, however, have a smaller land footprint and could also be used for final effluent polishing. Recycled materials have the potential to be used as filter media in bioretention applications for stormwater runoff treatment to abate with nutrient loads (Guo et al., 2015; Seelsaen et al., 2006). Filter media performance varies with the layer type, depth, surface area

of the materials, vegetation, pollutant concentration, and flow conditions (Eckart et al., 2017). Bioretention cells with recycled concrete aggregates (RCA) and rice husks (RH) have demonstrated promising results in stormwater-treatment studies. For example, 80–90% phosphate removal was achieved in batch tests with concrete aggregates (Deng and Wheatley, 2018; Ramsey et al., 2018). Rice husks have been used as constructed wetland media and achieved around 45% NH_3-N removal via ammonia-oxidizing bacteria (Tee et al., 2009). We also previously used rice husks and recycled concrete aggregates to assess their applicability in low nutrient, low flow, microorganism-free stormwater conditions where we separately filtered nitrate, nitrite, and phosphate from synthetic stormwater (Alam et al., 2021, 2022). Nevertheless, the performance of recycled media for wastewater effluent polishing, with higher concentrations of multiple nutrients and microbial levels in anammox effluent, has yet to be determined.

There is a critical need to improve nutrient removal polishing from anammox effluent prior to discharge because of impacts to receiving waters from remaining eutrophication potential (Preisner et al., 2020).

Additionally, recycled materials have demonstrated promising results in stormwater management and thus could be good candidates to be used in biofilters or sorptive filters for WWTP effluent polishing. Therefore, the objective of this study was to compare the fates, adsorption dynamics, and removal rates of common forms of nitrogen and phosphorus nutrients in rice husk and recycled concrete aggregate filter media. We hypothesized that the presence of divalent cations and metal hydroxides in concrete aggregates would yield higher phosphate adsorption than rice husks. Furthermore, we predicted that the presence of nutrients and organic carbon in rice husk would facilitate biotransformation and adsorption of nitrogen species, resulting in concomitantly higher nitrogen removal than concrete aggregates. In this study, we created a lab-scale 1.5 L sequencing batch anammox reactor fed with synthetic wastewater, representing sewage sludge dewatering effluent. We passed the reactor effluent through three separate columns: an RCA column, an RH column, and a two-stage column (50% RCA and 50% RH). The two-stage column demonstrated consistent removal for all the nutrients and exhibited the highest ammonia, nitrite, and nitrate removal performance. To the best of our knowledge, this is the first study to test the use of recycled materials, more commonly applied as media in stormwater bioretention, for downstream anammox effluent polishing treatment. Because treating pollutants from non-point sources can be difficult, improving point-source removal efficiency through innovative effluent polishing techniques will improve water reuse practices (Scholes et al., 2021).

2. Methods and materials

2.1. Synthetic wastewater and columns

The influent recipe for the anammox reactor was adapted from van de Graaf et al. (Van de Graaf et al., 1996). The influent consisted of two trace solutions (compositions in Table S1), 30.6 g/L $MgSO_4 \cdot 6H_2O$, 13.6 g/L $CaCl_2$, 0.0272 g/L KH_2PO_4 , 0.33 g/L $(NH_4)_2SO_4$, 0.345 g/L $NaNO_2$, and 0.5 g/L $KHCO_3$, where $(NH_4)_2SO_4$ and $NaNO_2$ were used to control the influent ammonium and nitrite ion concentrations, respectively. A continuous supply of influent to the reactor was ensured (Fig. S1). All chemicals were purchased from Sigma Aldrich (Table S1). All column materials (i.e., the clear cast acrylic tube and the fittings) were thoroughly cleaned with soap and water, then air-dried before assembly. The media materials were also thoroughly rinsed with deionized water and

air-dried to remove additional debris attached to the materials. The inside diameter of all the columns were 9.53 cm (3.75"). The bottom and top portions of all the columns were filled with 2.54 cm (1.0") and 1.27 cm (0.5") layers of gravel for drainage. In both the RCA and RH columns, 20.32-cm (8-inch) layers of materials were used. For the two-stage column, one 10.16 cm (4.0") layer of recycled concrete aggregates (top layer), and one 10.16 cm (4.0") layer of rice husks (bottom layer) were used. No media compaction was conducted for any of the columns. Mesh fabric strainers were placed in between each layer to prevent the displacement of the materials and blockage. All the columns were operated in down-flow mode and there was no evidence of flow short-circuiting (conservative tracer breakthrough curves shown in Fig. S7, Fig. S8, and Fig. S9). The recycled concrete aggregates were provided by Innovative Block of South Texas Ltd, Brownsville, Texas and the rice husks were from Peaceful Valley Farm Supply, Grass Valley, California. The densities of RCA and RH samples were measured as 1.150 g/cm³ and 0.163 g/cm³, and the hydraulic conductivities were 0.476 cm/s (moisture content = 38%) and 0.294 cm/s (moisture content = 61%), respectively (in an uncompacted condition).

2.2. Tracer test

Tracer tests were performed for all three columns using a sodium bromide (NaBr) solution to measure the advection and dispersion of influent through the columns. A 1-L NaBr solution (20 mg/L) was passed through the columns at a flow rate of 1 mL/s. Samples were collected from the end of the column every 20 s for the first 3 min and every 2 min thereafter. Ion chromatography (Dionex ICS 5000) was used to measure samples and calibration standards (1.25 mg/L, 2.50 mg/L, 5.0 mg/L, 10 mg/L and 20 mg/L NaBr prepared from 100 mg/L stock solution). Hydraulic properties of the columns (i.e., hydraulic conductivity, porosity, and retention time) and transport properties (i.e., superficial pore velocity and dispersion), were also calculated. The following equation was used to model the advection and dispersion in the column (Singh, 2002).

$$\frac{C}{C_0} = 0.5 \operatorname{erfc} \left(\frac{x - ut}{2\sqrt{\alpha ut}} \right) \quad \text{Equation 2}$$

where C_0 = Initial concentration, C = Effluent concentration, x = Column length, u = Superficial pore velocity, α = Dispersivity and t = Time. We plotted both the model data and actual test data in C/C_0 vs time graph, then calculated the pore velocity and dispersivity to determine the lowest difference between the model and experimental values.

2.3. Column isotherm experiment

Column isotherm experiments were conducted to measure the adsorption capacity of the recycled materials when there was only one nutrient present in the influent. For the first experiment, six 500 mL solutions were prepared with known concentrations of phosphate ions (5 mg/L, 10 mg/L, 20 mg/L, 30 mg/L, 40 mg/L, and 50 mg/L). All the solutions were passed through the column, and the effluent ion concentrations were measured. The same experiment was repeated for nitrite and nitrate ions. The measured influent and effluent ion concentrations were entered as linearized and non-linearized versions of Langmuir and Freundlich isotherm equations and the isotherm coefficients were calculated.

2.4. Reactor-column experimental design

The bench-scale anammox reactor had one mechanical stirrer, one heating tape, and three ports for the influent pipe, the effluent pipe, and the overflow prevention pipe. The reactor was covered by thermal insulation material. The seed sludge for the anammox reactor was collected from the DEMON HRSD York River Treatment Plant (Seaford, Virginia). The operating temperature of the reactor was set at 25 ± 2 °C

and continuous mixing was ensured by maintaining the stirrer at 120 revolution/minute (rpm). The synthetic wastewater was pumped into the reactor at a flow rate of 51.25 mL/min for 16 min. The retention time of the influent was 6 h, and the stirrer was programmed to turn off 15 min before effluent pumping to allow for biomass settling. The anammox effluent was pumped out and then passed through the columns at a flow rate of 60 mL/min (higher than typical stormwater biofilters (Beach et al., 2005), which are around 10–25 mL/min). The on/off initiation for the stirrer, the heating tape, the influent pump, and the effluent pump were controlled using a circuit timer (ChronTrol XT Series Circuit Timer). Each column was connected to the anammox reactor for three weeks and data were collected every seven days. A Hach DR1900 portable water spectrophotometer was used to measure the total N and ammonia concentration, and ion chromatography (Dionex ICS 5000) was used to measure NO_3^- , NO_2^- and PO_4^{3-} ion concentrations. The reactor and the column were considered as one single unit with two phases, where phase-1 included the influent tank, influent pump, and reactor and phase-2 included the effluent pump, column, and effluent tank.

2.5. Hydrus 1-D model

Hydrus 1-D software, a finite element model (PC-Progress, Prague, Czech Republic), was used to determine the adsorption isotherm coefficient, K_d , and the first-order reaction rate constant, k , during nutrient removal by the columns. This software can simulate one-dimensional solute transport through porous media using modified Richards equation and advection-dispersion equation (Li et al., 2018). To understand the Hydrus-1D predicted reaction rate, a separate experiment was conducted wherein 840 mL of the anammox effluent was pumped through each of the three columns at a flow rate of 1 mL/s. The column effluents were collected every 30 s and were analyzed via ion chromatography. This temporal column effluent concentration data was one of the inputs in the Hydrus model inputs. The columns were modeled in Hydrus 1-D software using column depth, hydraulic conductivity, superficial pore velocity, dispersivity, influent, and effluent nutrient concentrations to obtain K_d and k .

2.6. Quality assurance and statistical methods

DI water was passed through the columns before every use until the electrical conductivities of the inflow and outflow water equilibrated. All sample data were collected and analyzed in triplicate. Blanks and rinses were used during ion chromatography. Any effluent not used immediately after the collection was stored in a refrigerator at 4 °C. DI water was used for every dilution. The model graphs were calibrated iteratively with experimental data and p-values, R^2 values, RMSE values, and Nash-Sutcliffe Coefficients were reported for each graph.

3. Results and discussion

3.1. Column characterization

The efficacy of filter media depends greatly on the filter hydraulic properties and the sorption capacities of the filter material (Hsieh and Davis, 2005). We characterized the column hydraulic properties to better understand transport dynamics, chemical attenuation and to use them as inputs for the 1-D model. The rice husk (RH) column had the lowest pore velocity (47.6% of RCA, and 88.4% of two-stage), and hydraulic conductivity; consequently, the RH column had the highest retention time (1.7 times higher than RCA, and 1.5 times higher than two-stage) [Table S4]. High hydraulic conductivity is an important characteristic for biofilters to facilitate infiltration (Hsieh and Davis, 2005), which is directly proportional to flow rate at a specific hydraulic gradient; thus, removal efficiencies tend to decrease when flow rate increases (Abbas, 2015; Shackelford, 2013). In conventional stormwater

biofilter columns, the hydraulic conductivities have been reported in previous studies as 827 cm/day (Beach et al., 2005) (fine sand), 7780 cm/day (Hsieh and Davis, 2005) (mulch, soil, and sand), and 9850 cm/day (Mijic et al., 2020) (sand with gravel); these values are 2.5–50 times less than the results measured in our study. Up-flow woodchip bioreactors are reported to have 177 to 1037 times lower hydraulic conductivity (33.6 cm/day, 81.6 cm/day, 197 cm/day) than the hydraulic conductivities measured in our columns, which helped support anoxic conditions for denitrifying bacteria (Halaburka et al., 2017). We used these results on the superficial pore velocity and dispersivity to model the columns in Hydrus-1D.

Sorption capacity is a function of mixing and electrostatic attraction between the adsorbent media and the chemical and is a critical parameter for any media (Ramsey et al., 2018; Kandasamy et al., 2009). The goal of the isotherm experiment was to quantify the adsorption capacities of the columns for each nutrient (nitrate/nitrite/phosphate) separately. For all three ions and columns, the non-linearized Langmuir model exhibited the best fit of the experimental data [$R^2 \geq 0.92$, Fig. 1], compared to the linearized Freundlich [$R^2 \geq 0.87$, Fig. S5, Table S2], linearized Langmuir [$R^2 \geq 0.18$, Fig. S4, Table S2], or non-linearized Freundlich [$R^2 \geq 0.92$, Fig. S6, Table S3] isotherm models. With the non-linearized Langmuir model, the RH column exhibited maximum nitrite sorption capacity, with a q_m value of 0.046 mg/g (11.5 times higher than RCA, and 1.5 times higher than two-stage). The RH column also had the highest nitrate sorption capacity, $q_m = 0.023$ mg/g (3.8 times higher than the RCA, and 1.4 times higher than the two-stage). In contrast, the RCA column exhibited the highest phosphate adsorption capacity, with a $q_m = 0.074$ mg/g (2.1 times higher than RH, and 5.3 times higher than two-stage). Two previous studies reported similar adsorption capacities (0.025 mg/g and 0.134 mg/g) for crushed concrete, but with higher retention times of 72 h and 1 h, respectively [Table 1] (Buriánek et al., 2014; Ramsey et al., 2018). Although the retention time in our study was substantially shorter (e.g., 51 s for RCA) and thus could support much greater infiltration rates, the PO_4^{3-} sorption capacity in our RCA column was still 0.074 mg/g. We also observed a similar trend for NO_3^- sorption (0.012 mg/g for RCA vs. 0.029 mg/g in Ramsey et al.) (Ramsey et al., 2018). Other researchers have reported similar results for total P adsorption capacities for other recycled materials (shale rock: 0.023–0.750 mg/g, sand: 0.117–0.165 mg/g, gravel: 0.026–1.700 mg/g, biochar: 1.80 mg/g, brick dust: 0.45 mg/g, clinker ash: 0.29 mg/g, peanut husk: 0.01 mg/g) (Gubernat et al., 2020). Commercial adsorbents, such as zeolite, have much higher P adsorption capacities (around 300 mg/g) but are also very costly (typical silver-exchanged zeolite costs \$514 to \$592 per 100 g) (Jiang et al., 2013; Vikrant et al., 2018).

3.2. Column performance

The two-stage column containing both recycled materials exhibited the greatest decrease in concentrations for nitrate-N, nitrite-N, and ammonia-N in the effluent. The anammox reactor upstream of the recycled media biofilter performed as expected for the duration of the experiment and removed approximately 80% of the total N, 90% of the ammonia-N, and nearly 100% of the nitrite-N, but the nitrate and phosphate concentrations increased. The nitrate-N concentration in the anammox reactor effluent was 9 times higher than its influent, and the phosphate concentration was 1.1–1.5 times higher (Fig. S2 and Fig. S3). The only appreciable removal in the RCA column was for phosphate (22%), where there was also a ~10% increase in total N and nitrite. Metal hydroxides present in concrete surfaces react with nitrate and produce nitrite (Hewlett et al., 2019), which likely drove the observed increase in nitrite concentration. Calcium nitrate is often used in concrete as antifreeze, which also might contribute to the total N increase in the RCA column effluent (Karagöl et al., 2013). Unlike the RCA column, the RH column demonstrated removal of all nutrients tested. The total N removal efficiency was 50% on the first day, with the average removal throughout the experiment at 36%. The RH column demonstrated constant ammonia-N removal of 80%. Initial nitrite-N and nitrate-N removal efficiencies were 30% and 60%, respectively, on the first day, with the average removal being 18% and 37%, respectively. In previous work, we used rice husks to filter synthetic stormwater (prepared in deionized water, no bacteria present) containing 4.5 mg/L nitrate-N (mass load = 13.8 mg), and the mass removal was 1.52 mg per kg of the column material for 1.6 mL/s inflow rate (Alam et al., 2022). In this experiment, even though the influent nitrate-N mass load was almost 1.5 times of the synthetic stormwater (mass load = 20.0 mg), the nitrate-N mass removal/media material was almost 9 times of the previous experiment (mass removal = 13.5 mg per kg of the column material), which likely occurred because a high number of bacteria were present in the anammox wastewater effluent to facilitate denitrification [calculations in Table S5]. The phosphate removal efficiency also decreased with time (first day = 60%; average = 45%). Like the RH column, the two-stage column also removed ~20–90% of different nutrients (~90% ammonia-N, ~80% nitrite-N, ~40% nitrate-N, ~30% phosphate, and ~20% total N) [Fig. 2]. The ammonia-N, nitrate-N, and nitrite-N removals in the two-stage column were 1.1, 1.5, 4.4 times higher, respectively, than the RH column, but the phosphate removal was lower at only 60% of the removal in the RH column [Fig. 2]. In another previous study, our team used recycled concrete aggregate (RCA) column and layered media (LM) column (containing recycled concrete aggregates, rice husks, and recycled crushed glass) to measure nitrite and nitrate removal from bacteria-free synthetic stormwater under intermittent flow conditions where the dry period did not exceed 4 days

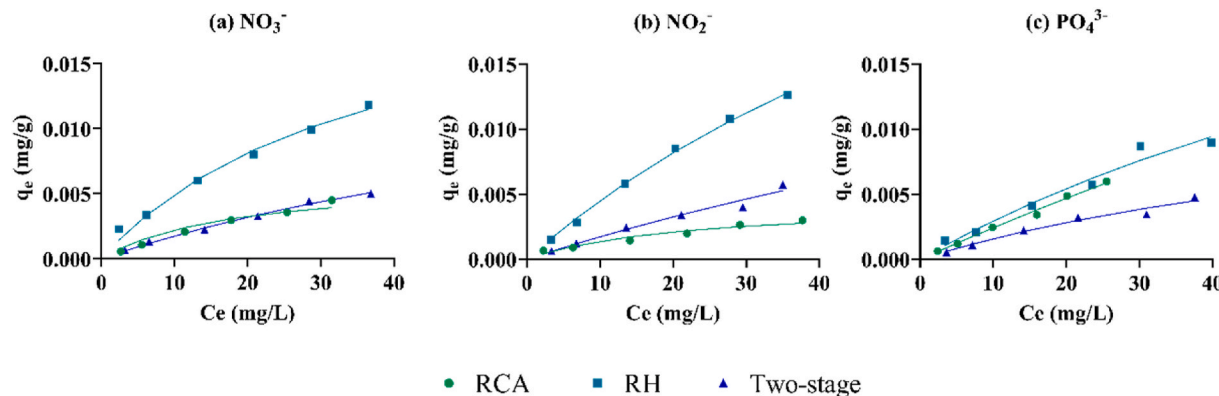


Fig. 1. Measured sorption isotherms for (a) nitrate, (b) nitrite, and (c) phosphate ions with each of the column media types [RCA = Recycled Concrete Aggregate, RH = Rice Husk, Two-stage = 10.16 cm (4") layer of recycled concrete aggregates (top layer) and 10.16 cm (4") layer of rice husks (bottom layer)]. Fitted values are presented via markings, model fits are presented via lines.

Table 1
Maximum adsorption capacities of different recycled media.

Materials	Nutrient	Isotherm Model	Residence Time	Result	Reference
Recycled Concrete Aggregate (RCA)	NO ₂ ⁻	Linearized Langmuir	51 s	q _m = 0.004 mg/g; K _L = 0.046 L/mg, r ² = 0.82	This Study
	NO ₃ ⁻	Linearized Langmuir	51 s	q _m = 0.012 mg/g, K _L = 0.018 L/mg, r ² = 0.95	
	PO ₄ ³⁻	Non-linearized Langmuir	51 s	q _m = 0.074 mg/g, K _L = 0.003 L/mg, r ² = 0.99	
Rice Husk (RH)	NO ₂ ⁻	Linearized Langmuir	85 s	q _m = 0.063 mg/g; K _L = 0.007 L/mg, r ² = 0.81	This Study
	NO ₃ ⁻	Non-linearized Langmuir	85 s	q _m = 0.023 mg/g; K _L = 0.028 L/mg, r ² = 0.99	
	PO ₄ ³⁻	Non-linearized Langmuir	85 s	q _m = 0.040 mg/g; K _L = 0.009 L/mg, r ² = 0.96	
50% RCA and 50% RH (by volume)	NO ₂ ⁻	Non-linearized Langmuir	56 s	q _m = 0.030 mg/g; K _L = 0.006 L/mg, r ² = 0.97	This Study
	NO ₃ ⁻	Non-linearized Langmuir	56 s	q _m = 0.017 mg/g; K _L = 0.011 L/mg, r ² = 0.99	
	PO ₄ ³⁻	Linearized Langmuir	56 s	q _m = 0.014 mg/g; K _L = 0.013 L/mg, r ² = 0.97	
Coarse Aggregate, Cement	PO ₄ ³⁻	Linearized Langmuir	72 Hours	q _m = 0.025 mg/g, K _L = 0.113 L/mg, r ² = 1	Ramsey et al. (2018)
	NO ₃ ⁻	Linearized Langmuir	72 Hours	q _m = 0.029 mg/g,	

Table 1 (continued)

Materials	Nutrient	Isotherm Model	Residence Time	Result	Reference
				K _L = 0.038 L/mg, r ² = 0.990	
Recycled Concrete	PO ₄ ³⁻	Linearized Langmuir	1 Hour	q _m = 0.134 mg/g	Buriánek et al. (2014)
Crushed Concrete	P	Empirical	40 Days	q _m = 8.3 mg/g	Egemose et al. (2012)
Rice Husk	Phenol	Linearized Langmuir	2 Hours	q _m = 0.002 mg/g, K _L = 30.72 L/mg, r ² = 0.87	Mahvi et al. (2004)
Sewage sludge-based activated carbon	Phenol	–	–	q _m = 0.9 mg/g	Björklund and Li (2017)

(Alam et al., 2021). The layered media column exhibited slightly higher average removal efficiencies than the recycled concrete aggregate column for both nitrite and nitrate (nitrite_{LM} = 26%, nitrite_{RCA} = 5%, nitrate_{LM} = 14%, and nitrate_{RCA} = 11%). Similar to the aforementioned work, denitrification was not considered, and the mass removal rate was lower than in this current work likely because bacteria present in the anammox effluent could facilitate some denitrification reactions. Using multiple layers in a biofilter is very common and improves filter performance. For example, sandy soil is used as the main filter media for conventional biofilters where a top mulch layer is added to increase infiltration, microbial degradation, and pollutant removal (Hsieh and Davis, 2005). Woodchips, tire crumbs, sawdust, and shredded paper have also been used in different layers of biofilters to increase efficiency (Ashoori et al., 2019; Halaburka et al., 2017, 2019; Wanielista et al., 2011). Similarly, incorporation of rice husks improved overall nutrient removal efficiencies in our two-stage column, as rice husks were able to remove more N-nutrients than the concrete aggregate. In summary, initial removal efficiencies for all the columns were higher than the average removal, which later stabilized, as is commonly reported for bioreactors (Addy et al., 2016).

The RCA column exhibited the fastest phosphate sorption reaction rate, likely due to the presence of metal hydroxides on the material surface (4.7 times higher than the two-stage column, and 104 times higher than the RH column) [Fig. 3]. Faster reactions will improve the successful implementation of a biofilter due to lesser required contact time. The Hydrus-1D model yielded the first-order reaction rate for nutrient removal considering the advection, diffusion, and reaction scenarios based on filter properties and temporal effluent nutrient concentrations (Meng et al., 2014). Because nitrite concentrations increased instead of decreasing, no modeling occurred for nitrite in the RCA column. In the RH column, faster reactions occurred for nitrite and nitrate removal than during phosphate removal (30 times greater reaction rate). For the two-stage column, the reaction rates for both nitrate and phosphate were 0.015 min⁻¹, but nitrite adsorption exhibited the fastest reaction (25 times higher reaction rate). The reaction rates in our study were similar to the reported rates for other commonly used filter media. For example, researchers have investigated the removal of N and P compounds using sawdust, soil, and sludge pyrolysis residue and report pseudo-first-order reaction rates of 0.028 min⁻¹ for nitrate, 0.051 min⁻¹ for nitrite, and 0.046–0.063 min⁻¹ for phosphate (Harmayani and Faisal Anwar, 2016; Yu et al., 2015). Mei et al. (2020) tested three media containing sand, iron powder, and aluminum powder for phosphorus

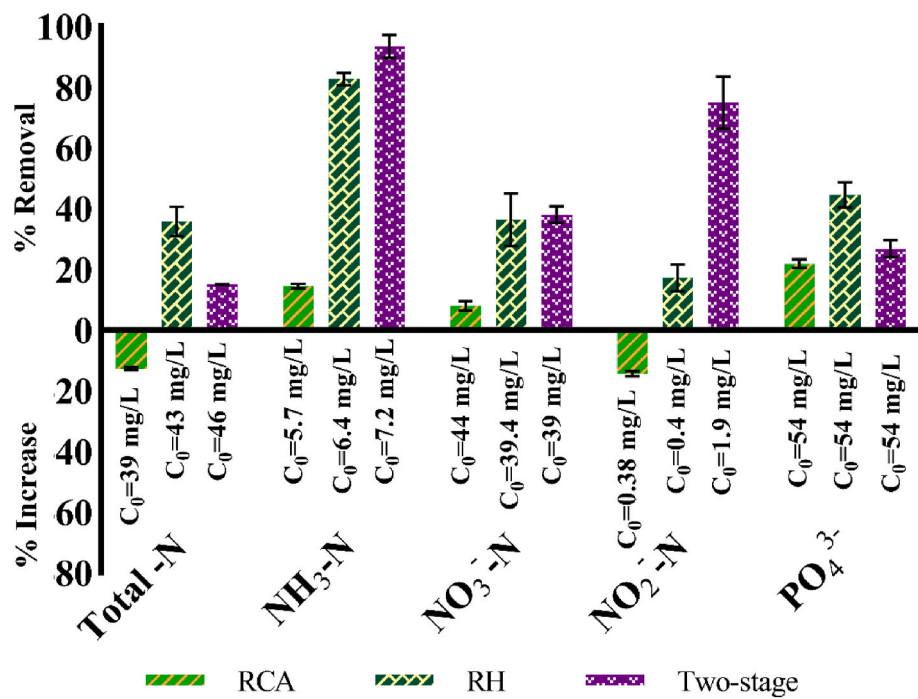


Fig. 2. Average nutrient removal in RCA, RH, and Two-stage columns (C_0 = column influent concentrations; the error bar represents the standard error of the mean, $n = 4$).

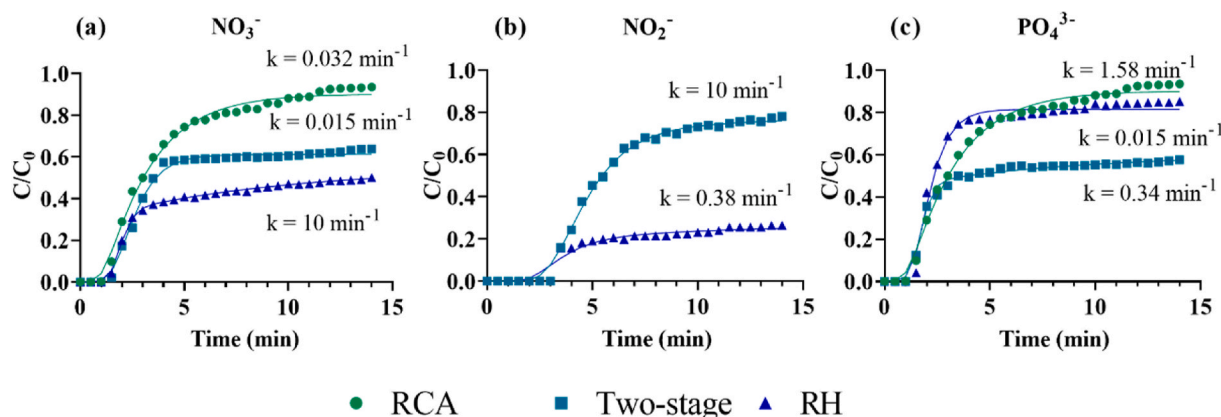


Fig. 3. Anammox effluent nutrient removal rates [pseudo-first order] through RCA, RH and Two-stage column (a) nitrate, (b) nitrite, (c) phosphate. Experimental values are presented via marked data points, Hydrus-1D model fits are presented via lines.

adsorption and reported second-order reaction rates of $0.058 \text{ Lmg}^{-1}\text{h}^{-1}$, $0.088 \text{ Lmg}^{-1}\text{h}^{-1}$, and $0.080 \text{ Lmg}^{-1}\text{h}^{-1}$ for sand, iron powder, and aluminum powder, respectively. First-order denitrification rates in a woodchip bioreactor spanned between 0.250 day^{-1} and 0.010 min^{-1} (DB et al., 2016; Lynn et al., 2015; Moorman et al., 2015; Robertson, 2010).

Nutrient removal in a biofilter heavily depends on the types, concentration, and number of nutrients, filter material, inflow rate, and removal mechanism (see Table 2). If nitrogen compounds are targeted for removal, media containing an organic carbon source, such as rice husk, woodchip, and sawdust can improve efficiency (Griebmeier and Gescher, 2018). Conversely, media containing metal hydroxides and silicon are better suited for phosphorus compounds removal (Mekonnen et al., 2020; Siwek et al., 2019). Improved phosphorus removal (39% or more) has been reported when the media contained cement (contains metal hydroxide and silicon), sand (contains silicon), and concrete (contains metal hydroxide). For example, Ramsey et al. reported 80% phosphate and 45–60% nitrate removal for concrete aggregate media

via adsorption (Ramsey et al., 2018). In contrast, Harmayani et al. reported 85–91% nitrate and 98% nitrite removals, respectively, in sawdust (Harmayani and Faisal Anwar, 2016). Most of these media were only tested using low influent concentrations ($\sim 2 \text{ mg/L}$ nitrate and 2 mg/L phosphate concentrations), which can impact removal efficiency. For example, Abbas investigated how phosphorus removal efficiency varies with influent concentration (Abbas, 2015). The removal efficiency decreased from 90% to 20% when the influent concentration increased from 1 mg/L to 100 mg/L (Abbas, 2015). Although the concentrations were higher in our experiments to more closely emulate anammox conditions (nitrate: $\sim 45 \text{ mg/L}$ and phosphate: $\sim 55 \text{ mg/L}$), our removal efficiencies matched what is commonly observed in bio-retention media ($\sim 38\%$ nitrate and $\sim 27\%$ phosphate removal in the two-stage column). If anoxic conditions were maintained in our columns, denitrification would likely increase the nitrate removal efficiency (Wang and Chu, 2016). The formation of a biofilm on the media surfaces would also likely further increase phosphate removal efficiency (Ning et al., 2015).

Table 2

Nutrient removal efficiencies in different recycled media.

Material	Major Components in Influent	Nutrient	Nutrient Load	Nutrient Removal	Mechanism	Reference
Recycled Concrete Aggregate (RCA)	EDTA, FeSO ₄ , ZnSO ₄ , CoCl ₂ , MnCl ₂ , CuSO ₄ , NaMoO ₄ , Na ₂ SeO ₄ , NiCl ₂ , H ₃ BO ₃ , MgSO ₄ , CaCl ₂ , KH ₂ PO ₄ , KHCO ₃ , (NH ₄) ₂ SO ₄ , NaNO ₂	Total N, NH ₃ -N, NO ₂ ⁻ -N, NO ₃ ⁻ -N, PO ₄ ³⁻	39.0 mg/L; 5.7 mg/L; 0.4 mg/L; 44.1 mg/L; 54.1 mg/L respectively	NH ₃ -N: 14.4%; NO ₃ ⁻ -N: 7.9%; PO ₄ ³⁻ : 21.8%	Adsorption	This study
Rice Husk (RH)	Same as RCA influent	Total N, NH ₃ -N, NO ₂ ⁻ -N, NO ₃ ⁻ -N, PO ₄ ³⁻	43.0 mg/L; 6.5 mg/L; 0.4 mg/L; 39.5 mg/L; 54.6 mg/L respectively	Total N: 35.8%; NH ₃ -N: 82.6%; NO ₂ ⁻ -N: 17.1%; NO ₃ ⁻ -N: 36.3%; PO ₄ ³⁻ : 44.5%	Adsorption	This study
50% RCA, 50% RH (by volume)	Same as RCA influent	Total N, NH ₃ -N, NO ₂ ⁻ -N, NO ₃ ⁻ -N, PO ₄ ³⁻	46.0 mg/L; 7.2 mg/L; 1.9 mg/L; 39.0 mg/L; 53.9 mg/L respectively	Total N: 15.0%; NH ₃ -N: 93.4%; NO ₂ ⁻ -N: 74.9%; NO ₃ ⁻ -N: 38.0%; PO ₄ ³⁻ : 26.7%	Adsorption	This study
Coarse aggregate, Cement	KH ₂ PO ₄	PO ₄ ³⁻ -P	0.2–2.4 mg/L	≥80%	Adsorption	Ramsey et al. (2018)
Coarse aggregate, Cement	KNO ₃	NO ₃ ⁻ -N	0.2–1.8 mg/L	45–60%	Adsorption	Ramsey et al. (2018)
Rice Husk (RH)	KH ₂ PO ₄	Total P	1–100 mg/L	20–90%	Adsorption	Abbas (2015)
Rice Husk (RH)	Phenol, NH ₃ -N	NH ₃ -N	Around 11–16 mg/L	0–45%	Nitrification	Tee et al. (2009)
62% sand, 32% soil, 6% mulch (by mass)	Na ₂ HPO ₄ , NaNO ₃ , NH ₄ Cl	NO ₃ ⁻ -N, NH ₃ -N, TP	2 mg/L, 2 mg/L, 3 mg/L respectively	TP: 39%, NO ₃ ⁻ -N: 4%, NH ₃ -N: 7%	Adsorption	Hsieh and Davis (2005)
25% Tire Crumb, 67.9% Sand, 7.1% Sawdust (by volume)	Different N and P ions	NO ₃ ⁻ , NH ₃ , Total N, PO ₄ ³⁻ , Total P	1.6 mg/L; 49.7 mg/L; 414 mg/L; 0.8 mg/L; 188 mg/L respectively	NO ₃ ⁻ : 97%; NH ₃ : 91.2%; Total N: 98.3%; PO ₄ ³⁻ : 98.8%; Total P: 99.9%	Adsorption; Denitrification	Wanielista et al. (2011)
25% Tire Crumb, 68.8% Sand, 6.2% Paper (by volume)	Different N and P ions	NO ₃ ⁻ , NH ₃ , Total N, PO ₄ ³⁻ , Total P	1.6 mg/L; 49.7 mg/L; 414 mg/L; 0.8 mg/L; 188 mg/L respectively	NO ₃ ⁻ : 90.1%; NH ₃ : 96.2%; Total N: 98.6%; PO ₄ ³⁻ : 97.8%; Total P: 99.9%	Adsorption; Denitrification	Wanielista et al. (2011)

Due to the presence of favorable macronutrients, such as cellulose and hemicellulose, rice husks tend to be a suitable biofilm carrier to facilitate microbial decomposition and can also remove nitrogen via electrostatic attraction, hydrogen bonds, or covalent bonds (Katal et al., 2012; Shao et al., 2009). Rice husks contain Ca, K, Mg, Na, Si, and P, which are essential (micro)nutrients for microbial metabolism and do not generally contain harmful heavy metals (Cu, Pb, Cd, Cr). In our study, dissolved oxygen concentrations of the filter influent and effluent were high (around 6.0 mg/L) and concomitant nitrate removal was less than what is commonly reported in denitrification bioreactors (dissolved oxygen in denitrifying woodchip bioreactors is ~0.5 mg/L (Halaburka et al., 2017)), thus we presumed denitrification inside the columns was minor. Nevertheless, there may have been localized denitrification, as has been observed in anoxic microsites in conventional bioretention cells (Willard et al., 2017). Nitrate sorption to biochar has also been reported, which negatively correlated with solution pH and positively correlated with biochar pyrolysis temperature (Fidel et al., 2018). Similar sorption onto rice husks might also account for some nitrate removal. If the column filter media had been operated favorable for anoxic conditions (i.e., sealed, compacted, and deep with a low flow), we may have observed denitrification inside the RH media column, likely increasing N removal efficiency (similar to a woodchip bioreactor) (Halaburka et al., 2017). One approach to promoting anoxic conditions in the RH column would be to increase the column packing density via compaction thereby decreasing flowrate and increasing contact time. The packing density of our air-dried rice husk in the RH column was 163 kg/m³ (concrete aggregate column = 1150 kg/m³), while the oven-dried packing density in typical woodchip bioreactors is around 200–285 kg/m³ (where denitrification is the main N removal mechanism) (Christianson et al., 2010). Packing densities for woodchip, pumice, small pebble, and cobblestone were reported respectively as 350 kg/m³, 390 kg/m³, 1750 kg/m³, and 1611 kg/m³, respectively, in a stormwater bioretention system (Niu et al., 2020). Nitrogen compound removal in concrete aggregate can occur via electrostatic attraction within concrete pores, physiochemical sorption to the concrete surface, or hydro/metal-nitrogen precipitation on the aggregate particles (Ramsey

et al., 2018). Recycled concrete aggregates contain Ca, Mg, Si, and Al hydroxides and phosphate react with Ca and Mg to form insoluble precipitates (MgHPO₄·3H₂O_(S), CaCO₃_(S), Ca₅(OH)(PO₄)₃_(S)) that aid phosphate removal (Deng and Wheatley, 2018). Phosphate removal on rice husks can involve attraction towards ligand functional groups present in the media and sorption to biofilms on the rice husk surface (Abbas, 2015; Ning et al., 2015). In our isotherm experiments, the RCA column demonstrated the highest phosphate sorption capacity while the RH column had higher nitrogen compound adsorption capacity. Among all the three columns, the two-stage column performance was greatest and most constant and shows promise for anammox effluent polishing; future work could consider adjustments to parameters such as flow rate, packing density, etc. to optimize nutrient removal.

3.3. Implications for application

Although we mainly discussed the use of rice husks and recycled concrete aggregates in the context of a downstream anammox polishing step, our results indicate the broader applicability of these recycled media. With the current setup, 14.8 mg nitrate-N and 14.4 mg phosphate can be removed per liter of the anammox effluent using the two-stage column, but long-term performance experiments with these media would be important for comprehensive understanding and application. Generally, the removal efficiency of sorptive media like bioretention or bioreactor systems decreases rapidly following the initial phase but stabilizes thereafter (stabilization rate varies with materials, setup, and influent conditions) (Halaburka et al., 2017). We observed similar trends in our study, with removal rates stabilizing after one week. Because nitrogen removal heavily depends on microbial activities, predicting the service life of a field-scale reactor from bench-scale experiments will likely be more variable (Waller et al., 2018). In contrast, phosphate removal occurs mainly via physiochemical sorption, and thus we can effectively estimate the field-scale treatment capacity of our current two-stage biofilter. If a small biofilter had a volume of 10 m³, it could treat around 7700 L of anammox effluent (~50 mg/L biofilter influent phosphate concentration, 26.7% removal rate) before

exhausting the sorption capacity [calculation in SI, 1.1 Treatment volume calculation]. Full-scale anammox plants in the field will have different flow rates and volumes, biofilters must be scaled accordingly. Phosphate concentrations in municipal WWTP effluent are much lower (Kermani et al., 2008; Wanielista et al., 2011) (around 0.5 mg/L, 100 times lower, nitrification-denitrification based process) than the anammox effluent used herein. If the above-mentioned two-step biofilter were used for municipal WWTP effluent polishing, around 325,000 L of effluent could be treated to remove phosphate. Eventually, the rice husk carbon source for microorganisms will be exhausted (estimated: 10–20 years); however, the overall biofilter service will be limited by sorption capacity (Björklund and Li, 2017). With longer retention time, greater depth, and/or lower flow rate, both N-P nutrient removal and total treated effluent volume should increase. The treatment volume would also increase if biofilm were to grow on the media and microbial degradation could recharge the adsorption capacities or sorption on the biofilm occurred. Thus, rice husks and recycled concrete aggregates as media in biofilters have the potential for application in field-scale stormwater, municipal WWTP, and anammox effluent polishing steps. Future research is needed to confirm their field-scale removal performance and service life by optimizing design and operation parameters (e.g., filter volume, flow rate, influent concentrations) (Abbas, 2015; Schmidt and Clark, 2013).

4. Conclusions

The anammox process is gaining popularity as an approach to treat high N-containing wastewater due to decreased energy demands. Nevertheless, anammox increases nitrate and phosphate concentrations in the effluent and thus effluent polishing can be highly beneficial. In this study, we integrated two recycled materials (rice husks and recycled concrete aggregates) as filter media to treat anammox process effluent. We have demonstrated that a two-stage biofilter (50% rice husk and 50% recycled concrete aggregate) can provide stable N and P nutrient removal from anammox effluent. Rice husks promoted N removal as a beneficial carbon source and biofilm carriers, whereas concrete aggregates removed phosphorus via sorption. Recycled materials in biofilters can improve effluent polishing because they are low energy, inexpensive, and practical to implement/maintain (De-Ville et al., 2021). Commercial media typically yield higher nutrient removal but are more costly and often harder to manage (Vikrant et al., 2018). Bioretention filter media amended with woodchips, shredded newspapers, biochar, vegetation, poultry litter, wheat straw, sawdust, and bottom ash from incineration plants are also reported to favorably remove nutrients (Osman et al., 2019; Sun et al., 2017; You et al., 2019). In future research, the long-term performance of a variety of recycled materials and their nutrient removal mechanisms should be investigated (i.e., variable flow, media density, influent pH, material refill frequency, material layer depth, and effluent recycling).

The use of recycled materials for biofilter media also improves environmental sustainability displacing these waste materials from landfills as well as improving effluent quality, lowering the operational cost, and providing a method for material reuse. Anammox is a growing technology, and it is expected to have large-scale implementations in wastewater and potentially stormwater treatment processes in the future. Adding a media biofilter following an anammox reactor as an effluent polishing step would help mitigate overall nutrient loads.

Credit author statement

Debojit S. Tanmoy: Conceptualization, Methodology, Software, Formal analysis, Investigation, Data curation, Writing – original draft, Visualization, Project administration, **Gregory H. LeFevre:** Resources, Writing – review & editing, Supervision, Project administration, Funding acquisition, **Juan C. Bezares-Cruz:** Conceptualization, Methodology, Resources, Supervision, Project administration, Funding

acquisition.

Declaration of competing interest

The authors declare that they have no known competing financial interests or personal relationships that could have appeared to influence the work reported in this paper.

Acknowledgments

JCB-C was supported by the project “Arroyo Colorado Watershed Protection Plan Implementation-Modeling and Maintenance Training of BMPs for Bacteria and Nutrient Uptake. Fiscal Year (FY) 2019, Clean Water Act (CWA), Section 319(h) Grant | Texas Commission on Environmental Quality (TCEQ)”. GHL was supported by the NSF CBET CAREER (1844720).

Appendix A. Supplementary data

Supplementary data to this article can be found online at <https://doi.org/10.1016/j.chemosphere.2022.134058>.

References

Abbas, M.N., 2015. Phosphorus removal from wastewater using rice husk and subsequent utilization of the waste residue. *Desalination Water Treat.* 55, 970–977.

Addy, K., Gold, A.J., Christianson, L.E., David, M.B., Schipper, L.A., Ratigan, N.A., 2016. Denitrifying bioreactors for nitrate removal: a meta-analysis. *J. Environ. Qual.* 45, 873–881. <https://doi.org/10.2134/jeq2015.07.0399>.

Alam, T., Bezares-Cruz, J.C., Mahmoud, A., Jones, K.D., 2022. Modeling transport, fate, and removal kinetics of nitrate and orthophosphate using recycled adsorbents for high and low-flow stormwater runoff treatment. *Chemosphere* 287, 132152. <https://doi.org/10.1016/j.chemosphere.2021.132152>.

Alam, T., Bezares-Cruz, J.C., Mahmoud, A., Jones, K.D., 2021. Nutrients and solids removal in bioretention columns using recycled materials under intermittent and frequent flow operations. *J. Environ. Manag.* 297, 113321. <https://doi.org/10.1016/j.jenvman.2021.113321>.

Ameta, S.C., 2018. Chapter 1 - introduction. In: Ameta, S.C., Ameta, R. (Eds.), *Advanced Oxidation Processes for Waste Water Treatment*. Academic Press, pp. 1–12. <https://doi.org/10.1016/B978-0-12-810499-6.00001-2>.

Ashoori, N., Teixido, M., Spahr, S., LeFevre, G.H., Sedlak, D.L., Luthy, R.G., 2019. Evaluation of pilot-scale biochar-amended woodchip bioreactors to remove nitrate, metals, and trace organic contaminants from urban stormwater runoff. *Water Res.* 154, 1–11. <https://doi.org/10.1016/j.watres.2019.01.040>.

Beach, D.N.H., McCray, J.E., Lowe, K.S., Siegrist, R.L., 2005. Temporal changes in hydraulic conductivity of sand porous media biofilters during wastewater infiltration due to biomat formation. *J. Hydrol.* 311, 230–243. <https://doi.org/10.1016/j.jhydrol.2005.01.024>.

Björklund, K., Li, L., 2017. Removal of organic contaminants in bioretention medium amended with activated carbon from sewage sludge. *Environ. Sci. Pollut. Res.* 24, 19167–19180. <https://doi.org/10.1007/s11356-017-9508-1>.

Brown, D.S., Kreissl, J.F., Gearheart, R.A., Kruzic, A.P., Boyle, W.C., Otis, R.J., 2000. *Manual - Constructed Wetlands Treatment of Municipal Wastewaters*. EPA, U.S.

Buriánek, P., Skálický, M., Grünwald, A., 2014. Phosphorus adsorption from water by recycled concrete. *Geosci. Eng.* 60, 1–8.

Christianson, L., Castelló, A., Christianson, R., Helmers, M., Bhandari, A., 2010. Technical note: hydraulic property determination of denitrifying bioreactor fill media. *Appl. Eng. Agric.* 26, 849–854. <https://doi.org/10.13031/2013.34946>.

Conley, D.J., Paerl, H.W., Howarth, R.W., Boesch, D.F., Seitzinger, S.P., Havens, K.E., Lancelot, C., Likens, G.E., 2009. Controlling eutrophication: nitrogen and phosphorus. *Science* 323, 1014–1015, 80.

Daverey, A., Su, S.-H., Huang, Y.-T., Chen, S.-S., Sung, S., Lin, J.-G., 2013. Partial nitrification and anammox process: a method for high strength optoelectronic industrial wastewater treatment. *Water Res.* 47, 2929–2937. <https://doi.org/10.1016/j.watres.2013.01.028>.

Db, J., Tb, M., Tb, P., Tc, K., 2016. Simulating woodchip bioreactor performance using a dual-porosity model. *J. Environ. Qual.* 45, 830–838. <https://doi.org/10.2134/jeq2015.07.0342>.

De-Ville, S., Green, D., Edmondson, J., Stirling, R., Dawson, R., Stovin, V., 2021. Evaluating the potential hydrological performance of a bioretention media with 100% recycled waste components. *Water* 13. <https://doi.org/10.3390/w13152014>, 2014.

Deng, Y., Wheatley, A., 2018. Mechanisms of phosphorus removal by recycled crushed concrete. *Int. J. Environ. Res. Publ. Health* 15, 357.

Dodds, W.K., Bouska, W.W., Eitzmann, J.L., Pilger, T.J., Pitts, K.L., Riley, A.J., Schloesser, J.T., Thornbrugh, D.J., 2009. Eutrophication of US freshwaters: analysis of potential economic damages. *Environ. Sci. Technol.* 43, 12–19.

Eckart, K., McPhee, Z., Bolisetti, T., 2017. Performance and implementation of low impact development–A review. *Sci. Total Environ.* 607, 413–432.

Egemose, S., Sønderup, M.J., Beinthon, M.V., Reitzel, K., Hoffmann, C.C., Flindt, M.R., 2012. Crushed concrete as a phosphate binding material: a potential new management tool. *J. Environ. Qual.* 41, 647–653.

EPA, U.S., 2009. National Lakes Assessment: A Collaborative Survey of the Nation's Lakes. U.S. Environmental Protection Agency, Office of Water and Office of Research and Development, Washington, D.C. (U.S. Environmental Protection Agency, Washington, D.C.).

Fidel, R.B., Laird, D.A., Spokas, K.A., 2018. Sorption of ammonium and nitrate to biochars is electrostatic and pH-dependent. *Sci. Rep.* 8, 17627. <https://doi.org/10.1038/s41598-018-35534-w>.

Gerba, C.P., Pepper, I.L., 2019. Chapter 22 - municipal wastewater treatment. In: Brusseau, M.L., Pepper, Ian L., Gerba, Charles, P. (Eds.), *Environmental and Pollution Science*. Academic Press, pp. 393–418. <https://doi.org/10.1016/B978-0-12-814719-1.00022-7>.

Griebelmeier, V., Gescher, J., 2018. Influence of the potential carbon sources for field denitrification beds on their microbial diversity and the fate of carbon and nitrate. *Front. Microbiol.* 9, 1313. <https://doi.org/10.3389/fmicb.2018.01313>.

Gubernat, S., Mastón, A., Czarnota, J., Koszelnik, P., 2020. Reactive Materials in the Removal of Phosphorus Compounds from Wastewater-A Review. <https://doi.org/10.3390/ma13153377>. Materials (Basel).

Gude, V.G., 2015. Energy and water autarky of wastewater treatment and power generation systems. *Renew. Sustain. Energy Rev.* 45, 52–68. <https://doi.org/10.1016/j.rser.2015.01.055>.

Guo, H., Lim, F.Y., Zhang, Y., Lee, L.Y., Hu, J.Y., Ong, S.L., Yau, W.K., Ong, G.S., 2015. Soil column studies on the performance evaluation of engineered soil mixes for bioretention systems. *Desalination Water Treat.* 54, 3661–3667. <https://doi.org/10.1080/19443994.2014.922284>.

Halaburka, B.J., Lefevre, G.H., Luthy, R.G., 2017. Evaluation of mechanistic models for nitrate removal in woodchip bioreactors. *Environ. Sci. Technol.* 51, 5156–5164. <https://doi.org/10.1021/acs.est.7b01025>.

Halaburka, B.J., LeFevre, G.H., Luthy, R.G., 2019. Quantifying the temperature dependence of nitrate reduction in woodchip bioreactors: experimental and modeled results with applied case-study. *Environ. Sci. Water Res. Technol.* 5, 782–797. <https://doi.org/10.1039/C8EW00848E>.

Harmayani, K.D., Faisal Anwar, A.H.M., 2016. Adsorption kinetics and equilibrium study of nitrogen species onto radiata pine (*Pinus radiata*) sawdust. *Water Sci. Technol.* 74, 402–415. <https://doi.org/10.2166/wst.2016.217>.

Hewlett, Peter Clive, Justnes, H., Edmeades, R.M., 2019. Cement and concrete admixtures. In: Hewlett, Peter C., Liska, M.B.T.-L.C. of C., Fifth, C.E. (Eds.), *Lea's Chemistry of Cement and Concrete*. Butterworth-Heinemann, pp. 641–698. <https://doi.org/10.1016/B978-0-08-100773-0.00014-9>.

Hsieh, C., Davis, A.P., 2005. Evaluation and optimization of bioretention media for treatment of urban storm water runoff. *J. Environ. Eng.* 131, 1521–1531.

Jasper, J.T., Jones, Z.L., Sharp, J.O., Sedlak, D.L., 2014. Biotransformation of trace organic contaminants in open-water unit process treatment wetlands. *Environ. Sci. Technol.* 48, 5136–5144. <https://doi.org/10.1021/es500351e>.

Jasper, J.T., Nguyen, M.T., Jones, Z.L., Ismail, N.S., Sedlak, D.L., Sharp, J.O., Luthy, R.G., Horne, A.J., Nelson, K.L., 2013. Unit process wetlands for removal of trace organic contaminants and pathogens from municipal wastewater effluents. *Environ. Eng. Sci.* 30, 421–436. <https://doi.org/10.1089/ees.2012.0239>.

Jasper, J.T., Sedlak, D.L., 2013. Phototransformation of wastewater-derived trace organic contaminants in open-water unit process treatment wetlands. *Environ. Sci. Technol.* 47, 10781–10790. <https://doi.org/10.1021/es304334w>.

Jiang, C., Jia, L., He, Y., Zhang, B., Kirumba, G., Xie, J., 2013. Adsorptive removal of phosphorus from aqueous solution using sponge iron and zeolite. *J. Colloid Interface Sci.* 402, 246–252. <https://doi.org/10.1016/j.jcis.2013.03.057>.

Kandasamy, J., Vigneswaran, S., Hoang, T.T.L., Chaudhary, D.N.S., 2009. Adsorption and biological filtration IN wastewater treatment. *Water Wastewater Treatment Technol.* 1, 173–204.

Karagöl, F., Demirboğa, R., Kaygusuz, M.A., Yadollahi, M.M., Polat, R., 2013. The influence of calcium nitrate as antifreeze admixture on the compressive strength of concrete exposed to low temperatures. *Cold Reg. Sci. Technol.* 89, 30–35. <https://doi.org/10.1016/j.coldregions.2013.02.001>.

Katal, R., Baei, M.S., Rahmati, H.T., Esfandian, H., 2012. Kinetic, isotherm and thermodynamic study of nitrate adsorption from aqueous solution using modified rice husk. *J. Ind. Eng. Chem.* 18, 295–302. <https://doi.org/10.1016/j.jiec.2011.11.035>.

Kermani, M., Bina, B., Movahedian, H., Amin, M.M., Nikaein, M., 2008. Application of moving bed biofilm process for biological organics and nutrients removal from municipal wastewater. *Am. J. Environ. Sci.* 4, 675. <https://doi.org/10.3844/ajessp.2008.675.682>.

Li, J., Zhao, R., Li, Y., Chen, L., 2018. Modeling the effects of parameter optimization on three bioretention tanks using the HYDRUS-1D model. *J. Environ. Manag.* 217, 38–46. <https://doi.org/10.1016/j.jenvman.2018.03.078>.

Lotti, T., Kleerebezem, R., Lubello, C., Van Loosdrecht, M.C.M., 2014. Physiological and kinetic characterization of a suspended cell anammox culture. *Water Res.* 60, 1–14.

Lynn, T.J., Yeh, D.H., Ergas, S.J., 2015. Performance and longevity of denitrifying woodchip biofilters for stormwater treatment: a microcosm study. *Environ. Eng. Sci.* 32, 321–330. <https://doi.org/10.1089/ees.2014.0358>.

Mahvi, A.H., Maleki, A., Eslami, A., 2004. Potential of rice husk and rice husk ash for phenol removal in aqueous systems. *Am. J. Appl. Sci.* 1, 321–326.

Maktabifard, M., Zaborowska, E., Makinia, J., 2018. Achieving energy neutrality in wastewater treatment plants through energy savings and enhancing renewable energy production. *Rev. Environ. Sci. Bio/Technol.* 17, 655–689. <https://doi.org/10.1007/s11157-018-9478-x>.

Mei, Y., Zhu, X.H., Gao, L., Zhou, H., Xiang, Y.J., Liu, F., 2020. Phosphorus adsorption/desorption kinetics of bioretention. *Therm. Sci.* 24, 2401–2410. <https://doi.org/10.2298/TSCI2004401M>.

Mekonnen, D.T., Alemeyehu, E., Lennartz, B., 2020. Removal of phosphate ions from aqueous solutions by adsorption onto leftover coal. *Water* 12, 1381. <https://doi.org/10.3390/w12051381>.

Meng, Y., Wang, H., Chen, J., Zhang, S., 2014. Modelling hydrology of a single bioretention system with HYDRUS-1D. *Sci. World J.* 521047. <https://doi.org/10.1155/2014/521047>, 2014.

Mijic, Z., Dayioglu, A.Y., Hatipoglu, M., Aydilek, A.H., 2020. Hydraulic and environmental impacts of using recycled asphalt pavement on highway shoulders. *Construct. Build. Mater.* 234, 117226. <https://doi.org/10.1016/j.conbuildmat.2019.117226>.

Moorman, T.B., Tomer, M.D., Smith, D.R., Jaynes, D.B., 2015. Evaluating the potential role of denitrifying bioreactors in reducing watershed-scale nitrate loads: a case study comparing three Midwestern (USA) watersheds. *Ecol. Eng.* 75, 441–448. <https://doi.org/10.1016/j.ecoleng.2014.11.062>.

Ning, Z., Liang, M., Wang, Z., Li, Y., Liu, Y., Wang, T., 2015. Nitrogen and phosphate adsorption on biofilms in reclaimed water. *Environ. Earth Sci.* 74, 451–461. <https://doi.org/10.1007/s12665-015-4053-z>.

Niu, S., Song, X., Yu, J., Kim, Y., 2020. Nitrogen reduction by fill-and-drain wetland receiving high pollution stormwater from impervious road generated by the initial precipitation. *Desalin. Water Treat.* 203, 150–159.

Osman, M., Wan Yusof, K., Takajudin, H., Goh, H.W., Abdul Malek, M., Azizan, N.A., Ab Ghani, A., Sa'Id Abdurrasheed, A., 2019. A review of nitrogen removal for urban stormwater runoff in bioretention system. *Sustainability* 11, 5415. <https://doi.org/10.3390/su11195415>.

Oulton, R.L., Kohn, T., Cwiertny, D.M., 2010. Pharmaceuticals and personal care products in effluent matrices: a survey of transformation and removal during wastewater treatment and implications for wastewater management. *J. Environ. Monit.* 12, 1956–1978. <https://doi.org/10.1039/c0em00068j>.

Piper, S., 2003. Impact of water quality on municipal water price and residential water demand and implications for water supply benefits. *Water Resour. Res.* 39, 1127. <https://doi.org/10.1029/2002WR001592>.

Preisner, M., Neverova-Dziopak, E., Kowalewski, Z., 2020. Mitigation of eutrophication caused by wastewater discharge: a simulation-based approach. *Ambio* 50, 413–424. <https://doi.org/10.1007/s13280-020-01346-4>.

Ramsey, A.J., Hart, M.L., Kevern, J.T., 2018. Nutrient removal rates of permeable reactive concrete. *J. Sustain. Water Built Environ.* 4, 4018004. <https://doi.org/10.1061/JSWBAY.0000850>.

Robertson, W.D., 2010. Nitrate removal rates in woodchip media of varying age. *Ecol. Eng.* 36, 1581–1587. <https://doi.org/10.1016/j.ecoleng.2010.01.008>.

Rosso, D., Larson, L.E., Stenstrom, M.K., 2008. Aeration of large-scale municipal wastewater treatment plants: state of the art. *Water Sci. Technol.* 57, 973–978.

Schmidt, C.A., Clark, M.W., 2013. Deciphering and modeling the physicochemical drivers of denitrification rates in bioreactors. *Ecol. Eng.* 60, 276–288. <https://doi.org/10.1016/j.ecoleng.2013.07.041>.

Scholes, R.C., Vega, M.A., Sharp, J.O., Sedlak, D.L., 2021. Nitrate removal from reverse osmosis concentrate in pilot-scale open-water unit process wetlands. *Environ. Sci. Water Res. Technol.* 7, 650–661. <https://doi.org/10.1039/DOWE0091C>.

Seelaesn, N., McLaughlan, R., Moore, S., Ball, J.E., Stuetz, R.M., 2006. Pollutant removal efficiency of alternative filtration media in stormwater treatment. *Water Sci. Technol.* 54, 299–305. <https://doi.org/10.2166/wst.2006.617>.

Shackelford, C.D., 2013. Geoenvironmental engineering. In: *Reference Module in Earth Systems and Environmental Sciences*. Elsevier. <https://doi.org/10.1016/B978-0-12-409548-9.05424-5>.

Shao, L., Xu, Z.X., Jin, W., Yin, H.L., 2009. Rice husk as carbon source and biofilm carrier for water denitrification. *Pol. J. Environ. Stud.* 18, 693–699.

Si, P., Li, J., Xie, W., Dong, H., Qiang, Z., 2021. Deciphering nitrogen removal mechanism through marine anammox bacteria treating nitrogen-laden saline wastewater under various phosphate doses: microbial community shift and phosphate crystal. *Bioresour. Technol.* 325, 124707. <https://doi.org/10.1016/J.BIOTECH.2021.124707>.

Singh, S.K., 2002. Estimating dispersion coefficient and porosity from soil-column tests. *J. Environ. Eng.* 128, 1095–1099.

Siwek, H., Bartkowiak, A., Włodarczyk, M., 2019. Adsorption of phosphates from aqueous solutions on alginate/goethite hydrogel composite. *Water* 11, 633. <https://doi.org/10.3390/w11040633>.

Sun, Y., Zhang, D., Wang, Z.W., 2017. The potential of using biological nitrogen removal technique for stormwater treatment. *Ecol. Eng.* 106, 482–495. <https://doi.org/10.1016/j.ecoleng.2017.05.045>.

Tee, H.C., Seng, C.E., Noor, A.M., Lim, P.E., 2009. Performance comparison of constructed wetlands with gravel-and rice husk-based media for phenol and nitrogen removal. *Sci. Total Environ.* 407, 3563–3571.

Toet, S., Van Logtestijn, R.S.P., Schreijer, M., Kampf, R., Verhoeven, J.T.A., 2005. The functioning of a wetland system used for polishing effluent from a sewage treatment plant. *Ecol. Eng.* 25, 101–124. <https://doi.org/10.1016/j.ecoleng.2005.03.004>.

Van de Graaf, A.A., de Brujin, P., Robertson, L.A., Jetten, M.S.M., Kuiken, J.G., 1996. Autotrophic growth of anaerobic ammonium-oxidizing micro-organisms in a fluidized bed reactor. *Microbiology* 142, 2187–2196.

Verlicchi, P., Masotti, L., Galletti, A., 2011. Wastewater polishing index: a tool for a rapid quality assessment of reclaimed wastewater. *Environ. Monit. Assess.* 173, 267–277. <https://doi.org/10.1007/s10661-010-1386-7>.

Vikrant, K., Kim, K.H., Ok, Y.S., Tsang, D.C.W., Tsang, Y.F., Giri, B.S., Singh, R.S., 2018. Engineered/designer biochar for the removal of phosphate in water and wastewater.

Sci. Total Environ. 616–617, 1242–1260. <https://doi.org/10.1016/j.scitotenv.2017.10.193>.

Waller, L.J., Evanyo, G.K., Krometis, L.-A.H., Strickland, M.S., Wynn-Thompson, T., Badgley, B.D., 2018. Engineered and environmental controls of microbial denitrification in established bioretention cells. Environ. Sci. Technol. 52, 5358–5366. <https://doi.org/10.1021/acs.est.7b06704>.

Wang, J., Chu, L., 2016. Biological nitrate removal from water and wastewater by solid-phase denitrification process. Biotechnol. Adv. 34, 1103–1112. <https://doi.org/10.1016/j.biotechadv.2016.07.001>.

Wanielista, M.P., Chang, N., Makkeasorn, A., 2011. Functionalized Green Filtration Media for Passive Underground Drainfield for Septic Tank Nutrient Removal. US7955507B2.

Willard, L.L., Wynn-Thompson, T., Krometis, L.H., Neher, T.P., Badgley, B.D., 2017. Does it pay to be mature? Evaluation of bioretention cell performance seven years postconstruction. J. Environ. Eng. 143, 04017041 [https://doi.org/10.1061/\(ASCE\)EE.1943-7870.0001232](https://doi.org/10.1061/(ASCE)EE.1943-7870.0001232).

Yamashita, T., Yamamoto-Ikemoto, R., 2014. Nitrogen and phosphorus removal from wastewater treatment plant effluent via bacterial sulfate reduction in an anoxic bioreactor packed with wood and iron. Int. J. Environ. Res. Publ. Health 11, 9835–9853. <https://doi.org/10.3390/ijerph110909835>.

Yang, X.-E., Wu, X., Hao, H.-L., He, Z.-L., 2008. Mechanisms and assessment of water eutrophication. J. Zhejiang Univ. - Sci. B 9, 197–209. <https://doi.org/10.1631/jzus.b0710626>.

You, Z., Zhang, L., Pan, S.-Y., Chiang, P.-C., Pei, S., Zhang, S., 2019. Performance evaluation of modified bioretention systems with alkaline solid wastes for enhanced nutrient removal from stormwater runoff. Water Res. 161, 61–73. <https://doi.org/10.1016/j.watres.2019.05.105>.

Yu, G., Zhang, B., Lu, X., Li, J., Chen, J., Zuo, J., 2015. Efficient removal of phosphorus in bioretention system by sludge pyrolysis residue. Arabian J. Geosci. 8, 3491–3499. <https://doi.org/10.1007/s12517-014-1462-3>.